

# NUMERICAL STUDY OF COOLING ENHANCEMENT: HEAT SINK WITH HOLLOW PERFORATED ELLIPTIC PIN FINS

Fatima Zohra BAKHTI<sup>1</sup>, Mohamed SI-AMEUR<sup>2</sup>

<sup>1</sup>University Med Boudiaf, Faculty of Technology, Mechanical Department 28000 M'sila, Algeria,  
fz\_bakhti@yahoo.fr

<sup>2</sup>University Hadj Lakhdar, Faculty of Technology, Mechanical Department  
LESEI/Avenue Chahid Boukhrouf Med Elhadi, 05000 Batna, Algeria, msiamour@yahoo.fr

## ABSTRACT

A mixed convective heat transfer in hollow perforated pin fins array with inline arrangement subject to a vertical impinging flow is numerically investigated. The governing equations based on Navier-Stokes equations are solved by adopting a three dimensional finite volume numerical model. The aim is to assess the thermal performance of the new heat sink (perforated pin fins) under several significant parameters such as geometrical position of the hole ( $h_t = 10, 20, 30, 40\text{mm}$ ) and the Reynolds number ( $Re = 50-500$ ). The effects of the height of horizontal hole and the vertical perforation on the thermal dissipation rate and the pressure drop are explicitly undertaken and compared to the standard configuration (without perforation).

**Keywords:** *cooling of the electronics components, perforated pin fins, elliptic hollow pin fins, mixed convection.*

---

## NOMENCLATURE

### Symbols :

$h_t$  height of horizontal hole, m

$H$  height of pin fin, m

$K_f$  heat thermal conductivity of the fluid, W/m.K

$K_s$  heat thermal conductivity of the solid, W/m.K

$L$  length of base plate, m

$\overline{Nu}$  the mean Nusselt number based on  $D_h (= \bar{h} \cdot D_h / K_f)$

$Q$  heat generated by the electronics component, W

$q_s$  heat generated per unit volume, W/m<sup>3</sup>

$Re$  Reynolds number ( $= \rho \cdot u_0 \cdot D_h / \mu$ )

$S_L$  longitudinal pitch, m

$S_T$  transversal pitch, m

$T_o$  inlet air temperature, K

$u, v, w$  velocity components in x, y, z directions

$u_0$  inlet air velocity, m/s

$W$  width of base plate, m

$w_b$  thickness of base plate, m

$w_s$  thickness of source volume, m

$x, y, z$  cartesian coordinates

### Greek Letters:

$\beta$  thermal expansion coefficient, 1/K

$\mu$  dynamic viscosity, Kg/m.s

$\nu$  kinematic viscosity ( $= \mu / \rho$ ), m<sup>2</sup>/s

$\rho$  the fluid density, Kg/m<sup>3</sup>

$\rho_o$  the fluid density at  $T_o$ , Kg/m<sup>3</sup>

---

## 1. INTRODUCTION

Enhancement of heat transfer surfaces has been developed over the years, and become the main focus in the heat exchanger industry. Extended surfaces or fins are an example of passive methods that are frequently used for enhancing heat transfer in heat exchanging devices for the purpose of increasing the heat transfer between a primary surface and ambient fluid. The use of perforated fins has been considered as one of the promising and useful methods in fins optimization. Sara et al. [1,2] indicated that the increase of different parameters relating

to the perforated blocks such as the perforation diameter, open area ratio, and the inclination of the perforations holes towards the surface of the plate improves heat transfer. The numerical results of Shaeri and Yaghoubi [3,4] show that the perforated longitudinal fins have a remarkable increase in heat transfer and reduced weight compared to solid fins. The studies of shaeri and Jen [5,6] is a complement of numerical investigation of Shaeri and Yaghoubi [4] to examine the effects of the size and number of perforations on the thermal characteristics of an array of perforated fins. Ismail [7] and Ismail et al. [8] indicated that the hexagonal perforated fins showed greater heat transfer enhancement performance, the circular perforated fins had slightly higher effectivity than the hexagonal perforated ones, and the triangular perforated fins had lowest skin friction coefficient value than the other types of fins considered. Al-Damook et al. [9] presented a numerical analysis of conjugate heat transfer from cylindrical fin pins with multiple circular, square and elliptic perforations. The results showed that the circular perforations provided the greatest enhancement in heat transfer and elliptical perforations minimize pressure drop.

## 2. NUMERICAL SIMULATION

A perspective view of the computational domain is shown in Figure 1. It consists of 14x7 of elliptic hollow fins arranged in an inline manner and attached to the upper surface of the common base plate. The dimensions of the base plate are  $L=W=164\text{mm}$  and  $w_b=12\text{mm}$ . Each hollow pin fin has semi-minor exterior and interior axis respectively equal 8 and 6mm and semi-major exterior and interior axis equal 12mm and 10mm and height  $H=81.6\text{mm}$ . The fins were perforated with the horizontal circular hole at the height  $h_t=10\text{mm}$ , 20mm, 30mm and 40mm from the bottom tip by  $d_t$  diameter equal 5mm. The longitudinal and transverse pitches are  $S_L=11.5\text{mm}$  and  $S_T=22.5$  respectively. Air passes through the heat sink as a coolant, thus taking away the heat generated in electronic component made from sillicium with the thickness  $w_s=10\text{mm}$  attached to the bottom of the heat sink and generates a quantity of heat  $Q=400\text{W}$ .

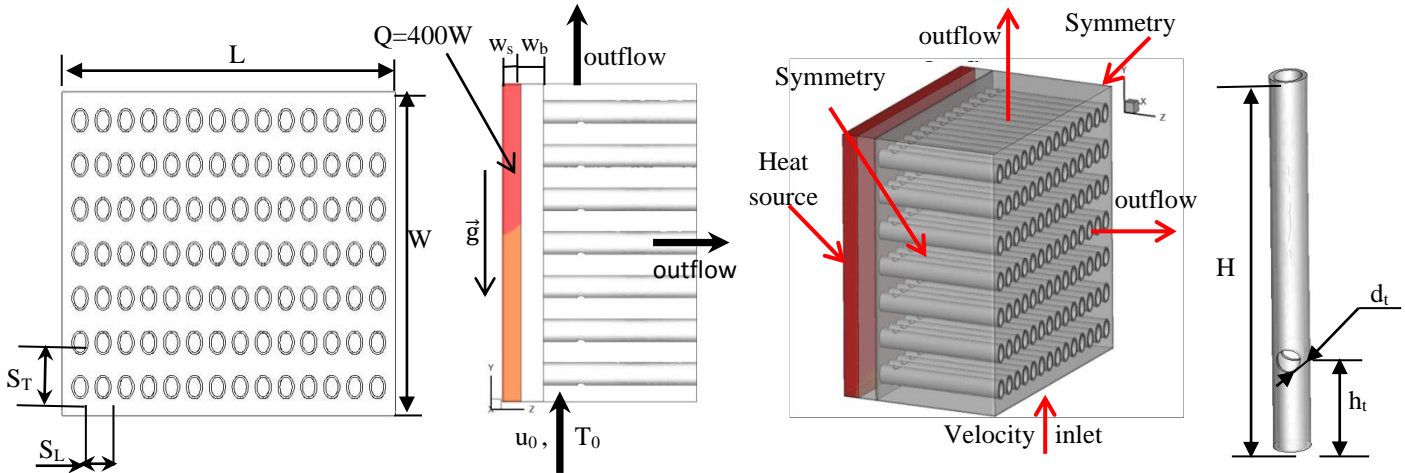


FIGURE 1. Designed geometry , Perspective view of the heat sink and a single perforated pin-fin configuration

The present study assumes that the flow is steady, laminar and 3D. The cooling fluid, which is air, is also assumed to be Newtonian and incompressible. All fluid thermo-physical properties are assumed uniform except for density in the buoyancy term, which is modeled using the Boussinesq approximation. Radiation is assumed to be negligible. The governing equations of conservation of mass, momentum and energy after applying the above assumptions are,

-Air side

*Continuity equation*

$$\frac{\partial u}{\partial x} + \frac{\partial v}{\partial y} + \frac{\partial w}{\partial z} = 0 \quad (1)$$

*x- Momentum equation.*

$$u \frac{\partial u}{\partial x} + v \frac{\partial u}{\partial y} + w \frac{\partial u}{\partial z} = -\frac{1}{\rho_0} \frac{\partial p}{\partial x} + \vartheta \left( \frac{\partial^2 u}{\partial x^2} + \frac{\partial^2 u}{\partial y^2} + \frac{\partial^2 u}{\partial z^2} \right) \quad (2)$$

*y- Momentum equation.*

$$u \frac{\partial v}{\partial x} + v \frac{\partial v}{\partial y} + w \frac{\partial v}{\partial z} = -\frac{1}{\rho_0} \frac{\partial p}{\partial y} + \vartheta \left( \frac{\partial^2 v}{\partial x^2} + \frac{\partial^2 v}{\partial y^2} + \frac{\partial^2 v}{\partial z^2} \right) + g\beta(T - T_0) \quad (3)$$

*z- Momentum equation.*

$$u \frac{\partial w}{\partial x} + v \frac{\partial w}{\partial y} + w \frac{\partial w}{\partial z} = -\frac{1}{\rho_0} \frac{\partial p}{\partial z} + \vartheta \left( \frac{\partial^2 w}{\partial x^2} + \frac{\partial^2 w}{\partial y^2} + \frac{\partial^2 w}{\partial z^2} \right) \quad (4)$$

*Energy equation*

$$u \frac{\partial T}{\partial x} + v \frac{\partial T}{\partial y} + w \frac{\partial T}{\partial z} = \frac{K_f}{\rho_0 c_p} \left( \frac{\partial^2 T}{\partial x^2} + \frac{\partial^2 T}{\partial y^2} + \frac{\partial^2 T}{\partial z^2} \right) \quad (5)$$

-Solid side

$$K_S \left( \frac{\partial^2 T}{\partial x^2} + \frac{\partial^2 T}{\partial y^2} + \frac{\partial^2 T}{\partial z^2} \right) + q_s = 0 \quad (6)$$

Where,  $K_f$  and  $K_S$  is the heat sink thermal conductivity respectively of the fluid and the solid,  $q_s$  is the heat generated per unit volume;

$$q_s = \frac{Q}{V}$$

$Q$  the heat generated by the electronic component ( $W$ ),  $V$  the volume of the electronic component ( $m^3$ )

-Boundary conditions

-Inlet flow condition (velocity-inlet)

$$u = w = 0, v = u_0, T = T_0 = 293.16K \quad (7)$$

-Outlet condition1: (Outflow), At plane ( $x, y=W, z$ )

$$\frac{\partial u}{\partial y} = \frac{\partial v}{\partial y} = \frac{\partial w}{\partial y} = \frac{\partial T}{\partial y} = 0 \quad (8)$$

-Outlet condition 2: (Outflow), At plane ( $x, y, z=H$ )

$$\frac{\partial u}{\partial z} = \frac{\partial v}{\partial z} = \frac{\partial w}{\partial z} = \frac{\partial T}{\partial z} = 0 \quad (9)$$

-At planes  $x = 0$  and  $x = W$ , we chose a symmetry conditions:

$$\frac{\partial u}{\partial x} = \frac{\partial w}{\partial x} = \frac{\partial T}{\partial x} = 0, v = 0 \quad (10)$$

-A heat source  $q_s$  is generated inside of the electronic component.

$$q_s = \frac{Q}{V} = 1487210W/m^3 \quad (11)$$

$$Q=400W, V=164 \text{ mm} \times 164 \text{ mm} \times 10 \text{ mm} = 268960 \text{ mm}^3$$

- The top surface of pin fin ( $z = H$ ) is well insulated.

- The contour of the base of the heat sinks and the electronics component are supposed to be adiabatic

-The heat flux between the interface of the fluid and the solid walls is coupled and its continuity between the interface of the solid and the liquid is given as:

$$K_S \cdot \frac{\partial T}{\partial n} \Big|_{\text{wall}} = K_f \cdot \frac{\partial T}{\partial n} \Big|_{\text{wall}} \quad (12)$$

The continuity, momentum and energy Equations (1)–(6) along with the boundary conditions (7)–(12) were solved numerically using a three-dimensional commercial CFD package, Fluent 6.3.26 which employs a finite volume method. A second-order upwind scheme was used to discretize the combined convection and diffusion terms in the momentum and energy equations. The SIMPLE algorithm was employed to solve the coupled pressure–velocity fields in the equations. The solution is assumed converged when the normalized residuals of the continuity and momentum equation fall below  $10^{-3}$  while that of the energy equation falls below  $10^{-6}$ .

### 3. RESULTATS AND DISCUSSIONS

Figure 2. shows temperature distribution through hollow/perforated elliptic pin fins, (a) at the horizontal plane going through the hole (b) at the middle section of the computational domain, i.e.  $x=0.075m$  and (c) for different height hole ( $h_t=10mm, 20mm, 30mm, 40mm$ ) and under the condition of  $Re = 250$ . From this figure it can be observed the fin temperature gradually increases in the direction of the flow due to the decrease in the velocity of flow and hence the cooling of the fins decrease.

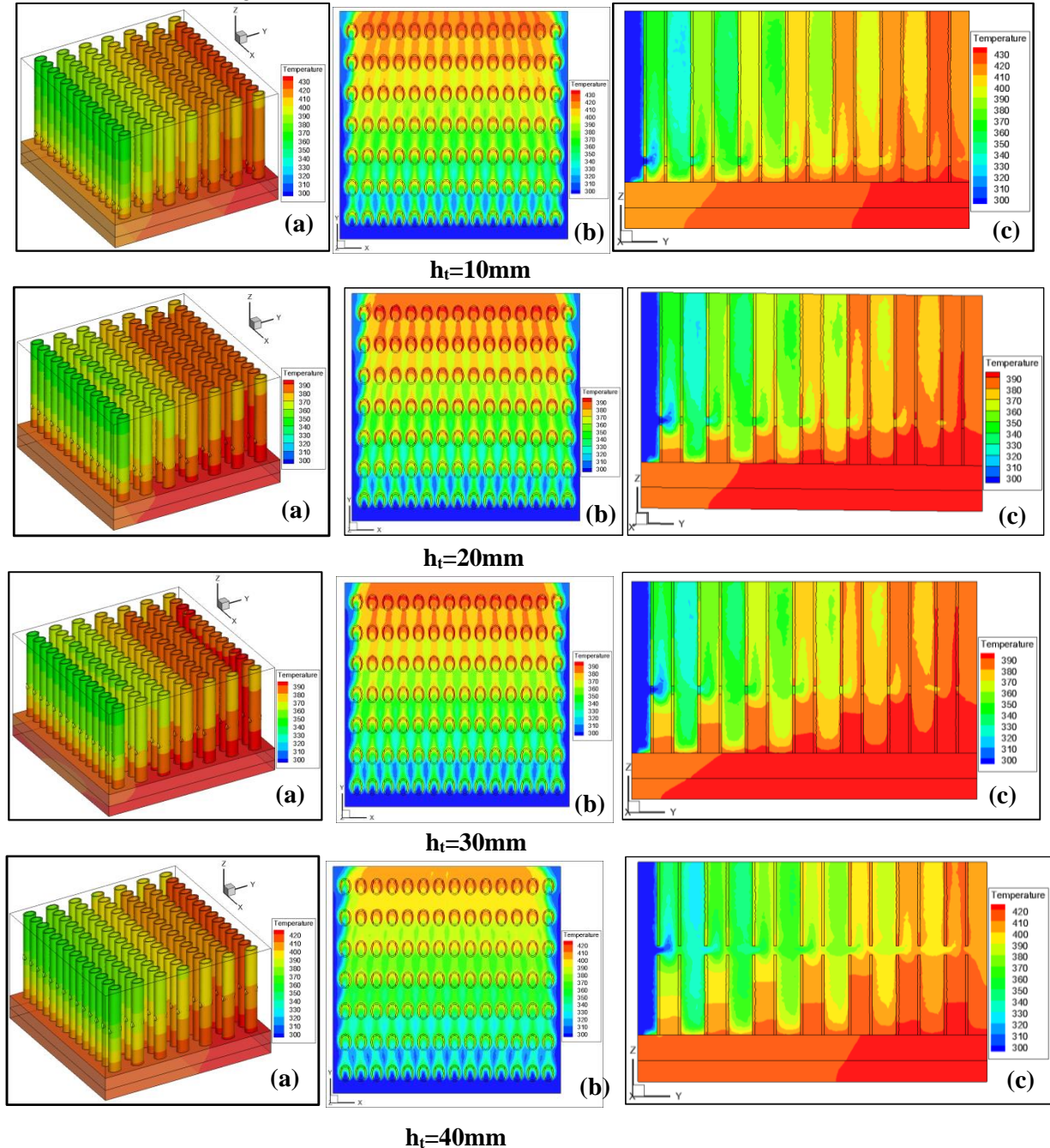


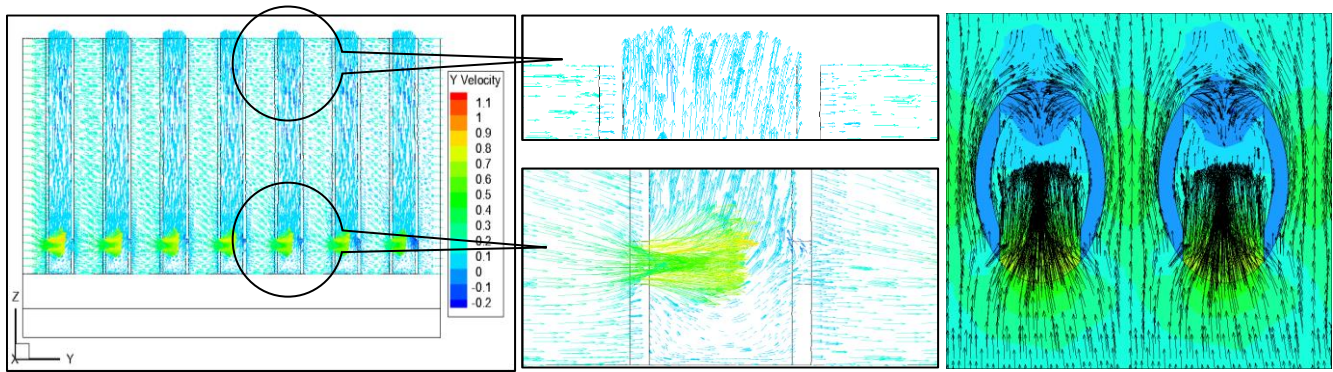
FIGURE 2. Contours of static temperature : (a) in the solid heat sink, (b) at the horizontal plane through the horizontal hole, (c) of the air at the middle of the sink at  $x = 0.075m$  for  $Re=250$ .

It is also seen that for different types of the fins the maximum temperature is at the fin base and it reduces to the tip because the fin takes the heat from the bottom heated plate thus taking away the heat generated by the electronic component. It is also seen that for different values of  $h_t$ , the fluid adjacent to the fins attains the maximum temperature, the fins take the heat from the bottom heated plate and the fluid takes away this heat



from the fins. Thus, the height value of the fluid temperature is observed at the bottom of the sink at the base plate and decreases as it moves along the height, the temperature difference between the fins and the surrounding fluid decreases along the height

Figure 3. (a) and (b) Show respectively the velocity vector fields at vertical plane  $x=0.075\text{mm}$  and on the horizontal plane going through the hole for height hole  $h_t=10\text{mm}$  and under the condition of  $Re = 250$ . As can be seen from this figures that the velocity profile of the air through the pin-fin heat sink with tends to be the same. The flow velocity profile shows that the air tends to flow through both sides of the pin-fins with a reduced velocity in regions between the pin-fins in the flow directions because of reduction of the space between the fins.



(a)

(b)

FIGURE 3. Velocity vectors for  $Re=250$  and  $h_t=10\text{mm}$  (a) in the plane  $x=0.075\text{m}$  (b) in the plane through the horizontal hole

A comparison of the variation of the average Nusselt number against Reynolds number for perforated hollow pin fins for various height hole and solid fins are shown in figure 4. From figure it is observed that for solid and perforated fins the Nusselt number increases with the increase of Reynolds number. It can be noted that the perforated fins yield the highest and the solid fins the lowest Nusselt number at all Reynolds numbers in the range considered here.

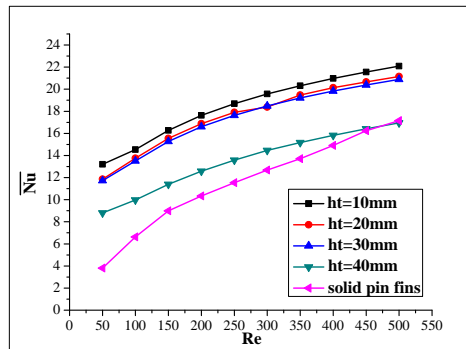


FIGURE 4. Variation of the mean Nusselt number according to Reynolds number

Perforated fins have a higher Nusselt number because, with introducing the perforation the area exposed to convection increased and increased interaction between fin and fluid, which increases the convective heat transfer. The perforated fins of  $h_t=10\text{mm}$  height of hole have the highest Nusselt number in comparison with the fins having  $h_t=20\text{mm}$ ,  $30\text{mm}$  and  $40\text{mm}$ . This is probably due to stronger interactions between the air flow that are in closer proximity of base of heat sink for  $h_t=10\text{mm}$  compared with other types of perforated pin.

#### 4. CONCLUSIONS

In this paper, 3D Numerical analysis of mixed convective heat transfer of solid fin arrays and new design hollow/ perforated elliptic fins four different heights of horizontal hole were carried. Calculations were carried out for a range of Reynolds numbers from 50 to 500 and height horizontal hole  $h_t=10\text{mm}$ ,  $20\text{mm}$ ,  $30\text{mm}$ ,  $40\text{mm}$ . The conclusions drawn from the present study may be summarized as:

- With the increase in Reynolds number the Nusselt number of solid and perforated fin increases.
- The enhancement in the heat transfer with perforated fins is higher than that with the solid fins as for whole tested range of Reynolds number and for all height of perforation.
- The perforated fins yield the highest and the solid fins the lowest Nusselt number at all Reynolds number.
- For perforated fins, with the decrease of the height of the hole, Nusselt number increase. The perforated fins of  $h_t=10\text{mm}$  height of hole have the highest Nusselt number in comparison with other value of height of the hole.

## REFERENCES

- [1] O.N. Sara, T. Pekdemir, S. Yapici, H. Ersahan. *Thermal performance analysis for solid and perforated blocks attached on a flat surface in duct flow. Energy Conversion and Management* 41, 1019-1028, 2000.
- [2] O.N. Sara, T. Pekdemir, S. Yapici, M. Yilmaz. Heat transfer enhancement in a channel flow with perforated rectangular blocks. *International Journal of Heat and Fluid Flow* 22, 509-518, 2001.
- [3] M.R. Shaeri, M. Yaghoubi. Numerical analysis of turbulent convection heat transfer from an array of perforated fins. *International Journal of Heat and Fluid Flow* 30, 218–228, 2009.
- [4] M.R. Shaeri, M. Yaghoubi. Thermal enhancement from heat sinks by using perforated fins. *Energy Conversion and Management* 50, 1264–1270, 2009.
- [5] Mohammad Reza Shaeri, Tien-Chien Jen. The effects of perforation sizes on laminar heat transfer characteristics of an array of perforated fins. *Energy Conversion and Management* 64, 328–334, 2012.
- [6] M.R. Shaeri, T.C. Jen, Turbulent heat transfer analysis of a three-dimensional array of perforated fins due to changes in perforation sizes. *Numerical Heat Transfer. Part A: Appl.* 61 (11) 16, 2012.
- [7] Md. Farhad Ismail. Effects of perforations on the thermal and fluid dynamic performance of a heat exchanger. *IEEE Transactions on Components, Packaging And Manufacturing Technology*, Vol. 3, No. 7, 2013.
- [8] Md. Farhad Ismail, Muhammad Noman Hasan, Suvash C. Saha. Numerical study of turbulent fluid flow and heat transfer in lateral perforated extended surfaces. *Energy* 64, 632-639, 2014.
- [9] Amer Al-Damook, J.L. Summers, N. Kapur, H. Thompson. Effect of different perforations shapes on the thermal-hydraulic performance of perforated pinned heat sinks. *Journal of Multidisciplinary Engineering Science and Technology (JMEST)*, Volume 3 Issue 4, 2016.